Propagation of broken stable beams

A. Cámara

▶ **To cite this version:**

A. Cámara. Propagation of broken stable beams. Journal of Modern Optics, 2011, 58 (9), pp.743. 10.1080/09500340.2011.573589 . hal-00687723

HAL Id: hal-00687723
https://hal.science/hal-00687723

Submitted on 14 Apr 2012

HAL is a multi-disciplinary open access archive for the deposit and dissemination of scientific research documents, whether they are published or not. The documents may come from teaching and research institutions in France or abroad, or from public or private research centers.

L'archive ouverte pluridisciplinaire **HAL**, est destinée au dépôt et à la diffusion de documents scientifiques de niveau recherche, publiés ou non, émanant des établissements d'enseignement et de recherche français ou étrangers, des laboratoires publics ou privés.

Journal of Modern Optics
Vol. 00, No. 00, 10 January 2010, 1–6

Propagation of broken stable beams

A. Cámara* and T. Alieva

Universidad Complutense de Madrid, Facultad de Ciencias Físicas
Ciudad Universitaria s/n, 28040 Madrid, Spain

(*March 2011*)

Beams that are stable during the propagation in a homogeneous and isotropic medium are widely used in optical particle manipulation, communication, metrology, etc. In real life scattering, absorption and diffraction by obstacles produce changes of the beam structure. The propagation of these *broken* beams is analysed. It is shown that, similary to the Bessel beams, they are able to reconstruct their original shape after being disturbed by obstacles of relatively small size.

Keywords: Gaussian beams; beam propagation; stable beams; fractional Fourier transform

1. Introduction

Paraxial stable beams, i. e., beams whose complex field amplitude remains unchanged during free space propagation apart from a scaling and an additional quadratic phase, are widely used in science and technology [1–6]. The well-known Hermite-Gaussian (HG), Laguerre-Gaussian (LG) [7], Hermite-Laguerre-Gaussian [8], and Ince-Gaussian beams [9] belong to this family. In general, any stable beam can be expressed as a linear combination of HG modes with constant sum of their indices. Apart from the Gaussian beam, the helical LG modes play a leading role in the applications mentioned above due to the axial symmetry and the carried orbital angular moment (OAM). In particular, they are used for micro-particle manipulation [1, 2], free space optics communications [3, 4], interferometric metrology [5], and atmosphere characterization [6]. It is worth mentioning that in the micro-particle manipulation the helical LG modes are able to induce a rotation of the trapped particles [2].

The propagation of stable beams through an inhomogeneous medium, as well as their interaction with particles in optical manipulation setups, lead to partial beam distortion. This fact may have negative consequences for trapping in multiple locations along the axial direction or for optical information transfer. Therefore, the self-reconstruction capacity becomes an important beam property for these applications. Furthermore, the study of the beam distortion provides information about the particle or medium characteristics and, therefore, the localization of the region with significant beam changes is also relevant. It has been shown in Refs. [10, 11] that non-diffracting Bessel beams as well as Bessel-Gaussian (BG) ones posses the self-recovering property. Here we study the regeneration capacity of stable scalar coherent beams after being distorted by obstacles simulated by simple models. We call these distorted beams *broken beams*.

*Corresponding author. Email: a.camara@fis.ucm.es

ISSN: 0950-0340 print/ISSN 1362-3044 online
© 2010 Taylor & Francis
DOI: 10.1080/0950034YYxxxxxxxx
http://www.informaworld.com

2. Theory

The propagation of paraxial beams in isotropic systems, including as a particular case the free space, is described by the symmetric fractional Fourier transform (FT) [12], apart from a scaling and an additional quadratic phase factor. The two-dimensional symmetric fractional FT of a complex field amplitude $f(\mathbf{r})$ for angle α is defined as

$$F^{\alpha}(\mathbf{r}) = \frac{1}{s^2|\sin\alpha|}\iint \mathrm{d}\mathbf{r}'\, f(\mathbf{r}') \exp\left\{\frac{\mathrm{i}\pi}{s^2}\left[\left(r^2+r'^2\right)\cot\alpha - 2\mathbf{r}\mathbf{r}'\csc\alpha\right]\right\}, \tag{1}$$

where $\mathbf{r} = (x, y)$ is the position vector, $r = |\mathbf{r}|$, and s is a normalizing parameter of units of length. The angle α associated with a free space propagation for a distance z is given by $\alpha = \arctan\left(z\lambda/s^2\right)$, where λ is the wavelength of the light source. We regard that the fractional FT for angle $\alpha = 0$ represents the original function, $f(\mathbf{r})$, while for $\alpha = \pi/2$ corresponds to the scaled FT which describes the far field diffraction.

The proper normalized stable beam is an eigenfunction for the fractional FT. Then, for the analysis of the broken beam evolution we consider its fractional FT for the angular parameter α ranging in the interval $[0, \pi/2]$. This way, the effective size of the beam remains unchanged providing a better visual comparison of the beam shape during the propagation.

In the projection approximation**,** three dimensional objects can be presented as plane obstacles characterized by a transmittance function $T(\mathbf{r})$. Thus, the broken beam $B(\mathbf{r}, 0)$ is given as a product between the stable beam $S(\mathbf{r})$ and $T(\mathbf{r})$: $B(\mathbf{r}, 0) = S(\mathbf{r})T(\mathbf{r})$, where

$$T(\mathbf{r}) = \begin{cases} 1, & \mathbf{r} \notin O(\mathbf{r}) \\ A(\mathbf{r})\exp\left[\mathrm{i}\varphi(\mathbf{r})\right], & \mathbf{r} \in O(\mathbf{r}) \end{cases}, \tag{2}$$

with $O(\mathbf{r})$ being the area of the obstacle. The fractional FT of $B(\mathbf{r}, 0)$ is written as

$$\begin{aligned} B(\mathbf{r},\alpha) &= \frac{1}{s^2|\sin\alpha|}\iint \mathrm{d}\mathbf{r}'\, S(\mathbf{r}')T(\mathbf{r}') \exp\left\{\frac{\mathrm{i}\pi}{s^2}\left[\left(r^2+r'^2\right)\cot\alpha - 2\mathbf{r}\mathbf{r}'\csc\alpha\right]\right\} \\ &= \frac{1}{s^2|\sin\alpha|}\exp\left(\frac{\mathrm{i}\pi r^2}{s^2}\cot\alpha\right)\iint \mathrm{d}\mathbf{r}'\, S(\mathbf{r}')T(\mathbf{r}')\exp\left[\frac{\mathrm{i}\pi}{s^2}\left(r'^2\cot\alpha - 2\mathbf{r}\mathbf{r}'\csc\alpha\right)\right]. \end{aligned} \tag{3}$$

We assume that $S(\mathbf{r})$ is an eigenfunction of the fractional FT defined **by Eq.** (1) for any angle α with eigenvalue C_α, and therefore, if there is no disturbance, i. e. $T(\mathbf{r}) = 1$, then $B(\mathbf{r}, \alpha) = C_\alpha S(\mathbf{r})$. Note that in this case the waist w of the enveloping Gaussian of the stable beam satisfies $w = s$.

Let us first discuss the beam reconstruction in the far zone, corresponding to $\alpha = \pi/2$. Using the fact that the FT of the product of two functions is the convolution between its FTs we obtain that the broken beam is transformed into

$$B(\mathbf{r}, \pi/2) = \tfrac{1}{s^2}\iint \mathrm{d}\mathbf{r}'\, S(\mathbf{r}')T(\mathbf{r}')\exp\left(-i2\pi\tfrac{\mathbf{r}\mathbf{r}'}{s^2}\right) = \tfrac{1}{s^2}C_{\pi/2}\iint \mathrm{d}\mathbf{r}'\, S(\mathbf{r}')\widehat{T}\left(\mathbf{r}-\mathbf{r}'\right), \tag{4}$$

where $\widehat{T}$ is the scaled FT of T and it has been taken into account that the stable beam is an eigenfunction for the FT with eigenvalue $C_{\pi/2}$. Therefore, the self-recovery of the broken beam

strongly depends on the form, position, and size of the obstacle. For very small obstacle size, $\widehat{T}(\mathbf{r})$ can be approximated by the Dirac delta function, which leads to a successful beam self-reconstruction. Increasing the area $O(\mathbf{r})$ results in a significant modification of the FT of the $B(\mathbf{r}, \pi/2)$ and, thus, produces worse beam recovery. The position of the obstacle controls the range of the filtered spatial frequencies. As it is well known, the low-frequency filtering (obstacle in the beam center) results in beam sharping, while the high-frequency elimination leads to beam smoothing. The form of the obstacle, which defines the range of the filtered spatial frequencies, is also important for the analysis of self-recovery.

For other fractional angles, the obstacle transmittance together with the chirp function $\exp\left(i\pi r^2 \cot\alpha/s^2\right)$, related to the Fresnel diffraction, are responsible for the beam filtering. The influence of the chirp function becomes neglectable for angles $\alpha > \alpha_c$, where α_c is defined from the condition that $O(\mathbf{r})$ belongs to the first Fresnel zone of radius $r = \sqrt{\lambda z/2} = s\sqrt{\tan\alpha_c/2}$. In this angular range the form of the beam coincides with the one in the far zone and, therefore, α_c indicates the distance of beam recovery. As we have already mentioned, the quality of the beam reconstruction depends on the obstacle parameters.

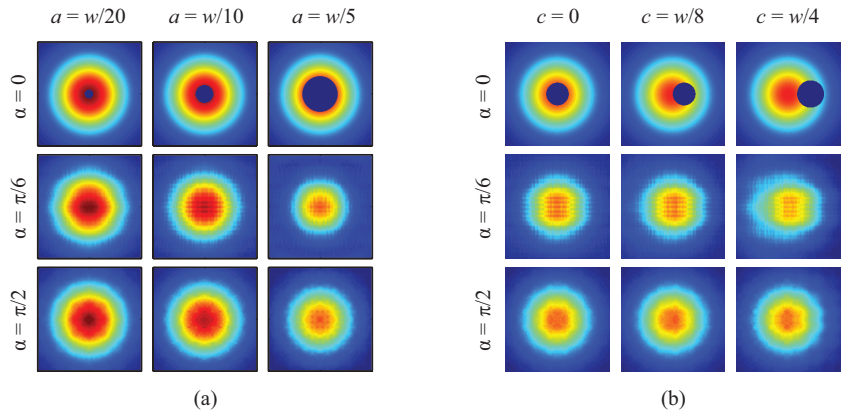

Figure 1. (Color on-line) Evolution for $\alpha = 0, \pi/6, \pi/2$ of the intensity distribution of the Gaussian beam disturbed by a circular mask. (a) Obstacles of different radius a are placed at the beam center. (b) Obstacles absorbing the same energy (8% from the total) are placed at different positions c.

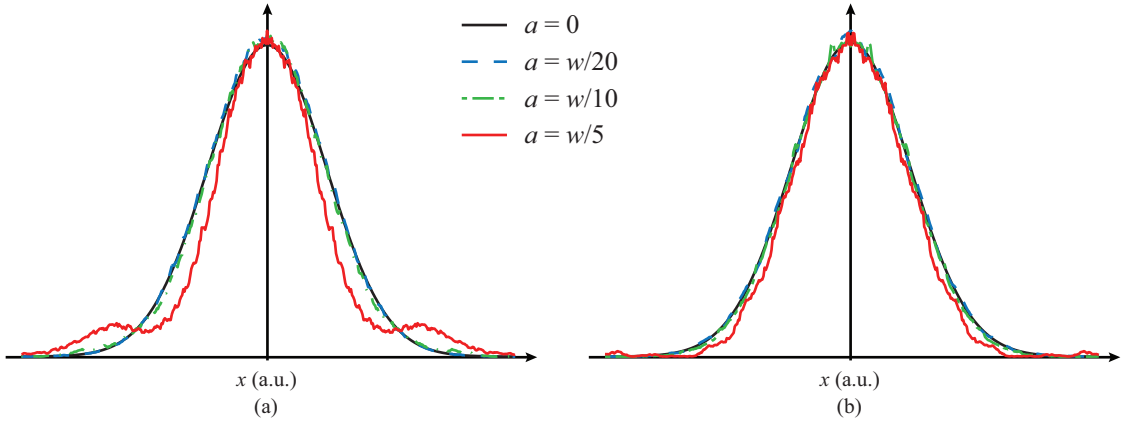

Figure 2. (Color on-line). Intensity profile along the x coordinate ($y = 0$) of the Gaussian beam disturbed by centered circular masks of different sizes for (a) $\alpha = \pi/6$ and (b) $\alpha = \pi/2$. The radius of the mask is $a = w/20, w/10, w/5$ for the dashed blue, dashed dotted green, and continuous red curves, respectively. The continuous black curve is the profile of the original Gaussian beam.

3. Numerical simulations

Our analysis is verified by the numerical simulations made for the Gaussian beams, disturbed by circular absorbing obstacles of different radii a and placed in different positions along the x axis, $\mathbf{c} = (c, 0)$. Thus, the obstacle function is

$$T(\mathbf{r}) = \begin{cases} 1, & \mathbf{r} \notin O(\mathbf{r}; a, c) \\ 0, & \mathbf{r} \in O(\mathbf{r}; a, c) \end{cases}, \tag{5}$$

and $O(\mathbf{r}; a, c) = \mathrm{circ}\left[(\mathbf{r} - \mathbf{c})/a\right]$, where

$$\mathrm{circ}(\mathbf{r}) = \begin{cases} 1, & r < 1 \\ 0, & r \geq 1 \end{cases}. \tag{6}$$

First we study the self-recovery of the Laguerre-Gaussian beam defined as

$$\mathrm{LG}^{l}{}_{p}(\mathbf{r}; w) = N_{\mathrm{LG}} L^{l}{}_{p}\left(2\pi \frac{r^2}{w^2}\right) \exp\left(-\pi \frac{r^2}{w^2}\right) \exp(il\theta), \tag{7}$$

where N_{LG} is a normalization constant, $L^{l}{}_{p}(\centerdot)$ is the Laguerre polynomial of radial index p and azimuthal index l, (r, θ) are the polar coordinates, and w is the beam waist. We remind that when $w = s$ the LG beam is an eigenfunction of the fractional FT [see Eq. (1)].

The self-reconstruction of the Gaussian beam ($\mathrm{LG}^{0}{}_{0}$) of waist $w = s$ distorted by circular masks of radius $a = w/20, w/10, w/5$ is displayed in Fig. 1(a), while the beam evolution for masks separated from the center distances $c = 0, w/8, w/4$ is shown in Fig. 1(b). Note that in the last case the energy absorbed by every obstacle is kept constant (8% from the total). It means that the mask radius varies depending on its position. We observe a successful beam recovery. This is also verified in Fig. 2, where we present the energy-normalized profiles along the x coordinate for $y = 0$ of the beam disturbed by centered masks of different sizes for two angles α corresponding to near ($\alpha = \pi/6$) and far ($\alpha = \pi/2$) field diffraction.

Let us now consider the evolution of a broken vortex beam. The propagation of the $\mathrm{LG}^{1}{}_{0}$ mode of waist $w = s$ is displayed in Fig. 3. As in the previous case, we consider the variation of the beam intensity distribution depending on the obstacle size $a = w/10, w/5, 2w/5$ [see Fig. 3(a)] and its position $c = 0, w/4, w/2$ [see Fig. 3(b)]. We observe that the LG beam is recovered faster for the smaller radius mask, while the bigger obstacle notably distorts the beam stability. Moreover, as it follows from Fig. 3(b), breaking the beam symmetry leads to worse beam reconstruction. The evolution of the intensity and phase distributions of the beam disturbed by a circular obstacle of radius $a = w/5$ placed at a maximum of its intensity distribution is displayed in Fig. 4. It is easy to check that the beam intensity and phase distributions qualitatively recover its forms for $\alpha > \pi/4$.

Finally, we compare the behavior of the LG beams with the Bessel ones. The Bessel beams are defined as $N_{\mathrm{B}} B_m(\beta r) \exp(im\theta)$, where N_{B} is a normalization constant, $B_m(\centerdot)$ is the Bessel function of order m, and β is a parameter related to the modulus of the transversal components of the plane wave vectors that compose the beam. As well as a plane wave, they are nondiffracting, but posses infinite energy. By adding a Gaussian envelope of waist w, the experimentally realizable Bessel-Gaussian (BG) beams are obtained [13]

$$\mathrm{BG}_{m,\beta}(\mathbf{r}; w) = N_{\mathrm{B}} B_m(\beta r) \exp\left(-\pi \frac{r^2}{w^2}\right) \exp(im\theta). \tag{8}$$

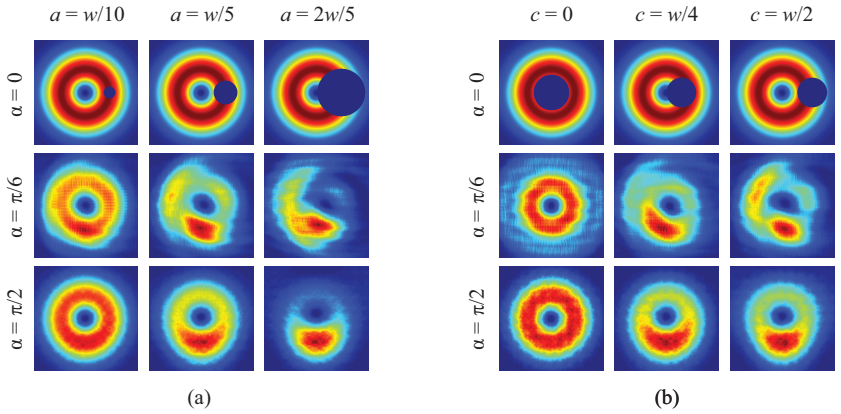

Figure 3. (Color on-line) Evolution for $\alpha = 0, \pi/6, \pi/2$ of the intensity distribution of the $LG^1{}_0$ beam disturbed by a circular mask. (a) Obstacles of different radius a are placed at the beam center. (b) Obstacles absorbing the same energy (8% from the total) are placed at different positions c.

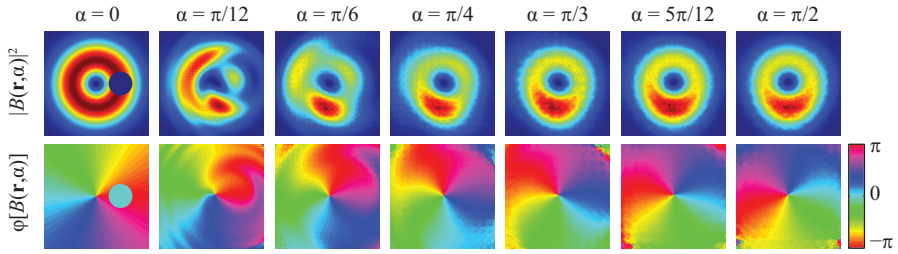

Figure 4. (Color on-line) Evolution for $\alpha \in [0, \pi/2]$ of the intensity and phase distributions of the $LG^1{}_0$ beam disturbed by a circular mask of radius $a = w/5$ placed at a maximum of intensity of the mode.

These beams are nondiffracting during the free space propagation in the range $z = [0, z_{\max}]$, where $z = 0$ coincides with the waist plane and $z_{\max} = 2\sqrt{\pi}w/(\lambda\beta)$ [10]. For convenience, we define a $\alpha_{\max}$ as the fractional FT parameter that corresponds to the propagation distance $z_{\max}$, i. e., $\alpha_{\max} = \arctan\left(z_{\max}\lambda/s^2\right)$.

As well as for the case of LG beams, the free space propagation of the obstructed BG beams is simulated using the symmetric fractional FT. In order to compare the behavior of the LG and BG beams we have chosen the beams with the same effective size defined by second-order intensity moments, m_{xx} and m_{yy}, and the same number of rings. We have verified that the evolution of the obstructed BG beam $BG_{1,1/s}$ is very similar to one of the LG mode $LG^1{}_0$ (see Fig. 4) with the same waist $w = s$, disturbed by the same obstacle. Changing the β and w parameters the BG beam $BG_{1,5/s}$ with two visible rings has been obtained. For the comparison, the LG mode $LG^2{}_1$ ($w = s$) with the same number of rings and effective size has been chosen. The evolution of the two distorted beams, $BG_{1,5/s}$ and $LG^2{}_1$, is shown in Fig. 5(a) and (b), respectively. The obstacles of the two beams are completely opaque circles, placed at the maximum of intensity in the positive x coordinate, and with radius such that they absorb 5% of the total energy of the beam. Since for the BG beam $\alpha_{\max} \lessapprox \pi/3$, we present the propagation of both beams for the interval $\alpha \in [0, \pi/3]$.

We observe that the behavior of the $BG_{1,5/s}$ beam is similar to the $LG^2{}_1$. Both recover they original intensity for a relative small distance, $\alpha = 2\pi/15$. Nevertheless, we underline that the BG beam starts diverging for $\alpha > 4\pi/15$, while the LG maintains its shape invariant.

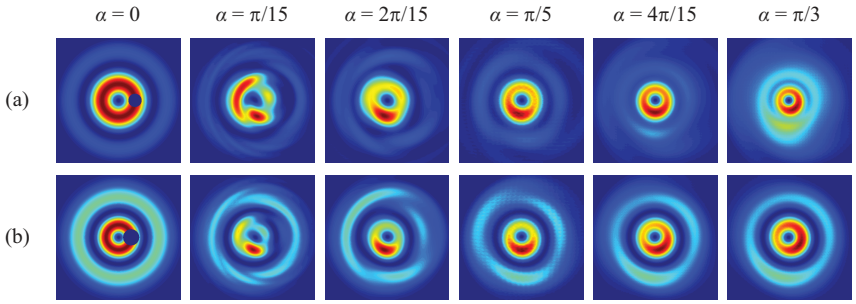

Figure 5. (Color on-line) Evolution of the intensity distribution of the obstructed $BG_{1,5/s}$ (a) and $LG^2{}_1$ (b) modes for $\alpha = [0, \pi/3]$. The waist of $LG^2{}_1$ is $w = s$ and the waist of $BG_{1,5/s}$ is such that both beams have the same apparent size (same second-order moments of intensity, m_{xx} and m_{yy}). The obstacles are opaque circles placed in the intensity maximum along the positive x coordinate that absorb 5% of the total energy.

4. Conclusions

We conclude that stable beams, as well as Bessel beams, posses the self-reconstructing property due to the invariance of their form during the propagation. This effect is easily explained by filtering theory. The simulation results indicate that the beam recuperation does not depend of the value of the beam OAM. Indeed, we observe that both beams, with the topological charge 0 ($LG^0{}_0$) and 1 ($LG^1{}_0$), show similar self-regeneration capacities after the distortion of the same percent of beam energy by an obstacle of the same form. The quality of the reconstruction is highly dependent on the obstacle parameters. We also note that other beams such as spiral [14] or auto reciprocal [15] ones are also able to recover their form after relatively small beam distortion as follows from a similar beam evolution analysis.

Acknowledgements

The financial support from the Spanish Ministry of Science and Innovation under project TEC2008-04105 is acknowledged. A. Cámara thanks the financial support from the Consejería de Educación de la Comunidad de Madrid and the European Social Fund. The authors are grateful to J.A. Rodrigo for the Matlab implementation of the fractional FT used for the simulations.

References

[1] A. Ashkin, J. M. Dziedzic, J. E. Bjorkholm, *et al.*, Opt. Lett. **11** 288 (1986).
[2] H. He, M. E. J. Friese, N. R. Heckenberg, *et al.*, Phys. Rev. Lett. **75** 826 (1995).
[3] M. D'Amico, A. Leva and B. Micheli, Microwave and Wireless Components Letters, IEEE **13** 305 (2003).
[4] G. Gibson, J. Courtial, M. Padgett, *et al.*, Opt. Express **12** 5448 (2004).
[5] S. Fürhapter, A. Jesacher, S. Bernet, *et al.*, Opt. Lett. **30** 1953 (2005).
[6] M. A. Molchan, E. V. Doktorov and R. A. Vlasov, Journal of Optics A: Pure and Applied Optics **11** 015706 (7pp) (2009).
[7] A. E. Siegman, *Lasers* (University Science Books, 1986).
[8] E. Abramochkin and V. Volostnikov, Optics Communications **83** 123 (1991).
[9] M. A. Bandres and J. Gutiérrez-Vega, Opt. Lett. **29** 144 (2004).
[10] Z. Bouchal, J. Wagner and M. Chlup, Optics Communications **151** 207 (1998).
[11] V. Garces-Chavez, D. McGloin, H. Melville, *et al.*, Nature **419** 145 (2002).
[12] H. M. Ozaktas, Z. Zalevsky and M. A. Kutay, *The Fractional Fourier transform with applications in optics and signal processing* (Wiley, New York, 2001).
[13] F. Gori, G. Guattari and C. Padovani, Optics Communications **64** 491 (1987).
[14] E. G. Abramochkin and V. G. Volostnikov, Physics-Uspekhi **47** 1177 (2004).
[15] T. Alieva and A. M. Barbé, Journal of Modern Optics **46** 8399 (1999).